Experimental Neurology 387 (2025) 115183

Contents lists available at ScienceDirect

Experimental Neurology

journal homepage: www.elsevier.com/locate/yexnr

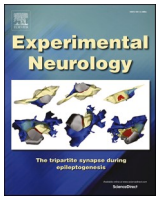

Research paper

Molecular and functional changes in GABAergic transmission during epileptogenesis in a rat model of post-traumatic epilepsy

Noora Puhakka [a], Pierangelo Cifelli [b], Gabriele Ruffolo [c,d], Alessandro Gaeta [c], Cristina Roseti [e,f], Angela Di Iacovo [e], Johanna Tiilikainen [a], Xavier Ekolle Ndode-Ekane [a], Anssi Lipponen [a,g], Meinrad Drexel [h], Günther Sperk [h], Asla Pitkänen [a,1,*], Eleonora Palma [c,i,1,**]

[a] A. I. Virtanen Institute for Molecular Sciences, University of Eastern Finland, PO Box 1627, FI-70211 Kuopio, Finland
[b] Department of Biotechnological and Applied Clinical Sciences (DISCAB), University of Aquila, 67100 Aquila, Italy
[c] Department of Physiology and Pharmacology, University of Rome, Sapienza, P.le Aldo Moro, 5, 00185 Rome, Italy
[d] IRCCS San Raffaele Cassino, Via Gaetano di Biasio, 1, 03043 Frosinone, Italy
[e] Department of Biotechnology and Life Sciences, Laboratory of Cellular and Molecular Physiology, University of Insubria, Varese, Italy
[f] Centre for Neuroscience, University of Insubria, Varese, Italy
[g] Institute of Biomedicine, University of Eastern Finland, PO Box 1627, FI-70211 Kuopio, Finland
[h] Department of Pharmacology, Medical University Innsbruck, Peter-Mayr-Str. 1a, 6020 Innsbruck, Austria
[i] IRCCS San Raffaele Roma, Via della Pisana, 235, 00163 Rome, Italy

ARTICLE INFO

Keywords:
GABAergic signaling
Cation-chloride cotransporter gene
Electrophysiology
Epileptogenesis
Traumatic brain injury

ABSTRACT

Traumatic brain injury (TBI) is one of the leading causes of structural epilepsy. Our objective was to investigate the molecular and functional dysregulation of GABAergic neurotransmission during a wide time window from acute to chronic phases of epileptogenesis after TBI. Perilesional and thalamic tissues sampled from a clinically relevant animal model of post-traumatic epilepsy induced by lateral fluid-percussion injury were investigated using *in situ* hybridization, immunohistochemistry and RNA sequencing. For functional analysis, we utilized a membrane microtransplantation technique in *Xenopus* oocytes in order to overcome the technical difficulties that would stem from recording directly from highly damaged lesional and perilesional brain tissues. Already at 6 to 24 h post-TBI we found a dysregulation in the expression of $GABA_AR$ β3- and δ-subunits, which persisted for up to 4 months. Further, gene set enrichment analysis revealed a negative enrichment of GABA receptor signaling in the perilesional cortex and ipsilateral thalamus. These changes occurred in parallel to the dysregulation of the two main cation-chloride cotransporter genes (*Slc12a2* and *Slc12a5*) both in the perilesional cortex and the ipsilateral thalamus. Our functional analysis revealed that the GABA current reversal potential (E_{GABA}) was shifted towards more depolarized values in the perilesional cortex and ipsilateral thalamus. Our data demonstrate a rapid onset and long-lasting duration of GABAergic dysfunction after TBI and support the hypothesis that an early treatment with agents modulating the GABAergic transmission in the thalamo-cortical-thalamic circuitry may suppress early seizures as well as prevent or slow down epileptogenesis after TBI.

1. Introduction

Traumatic brain injury (TBI) refers to an alteration of brain function caused by an external force (Dulla and Pitkänen, 2021). It is one of the leading causes of structural epilepsy (Dulla and Pitkänen, 2021). Furthermore, patients with post-traumatic epilepsy (PTE) are frequently refractory to treatment with anti-seizure medications (ASMs) and report a significant decrease in their quality of life (Dulla and Pitkänen, 2021). Unlike in many other forms of epilepsy, in cases of PTE the time of initiation of the epileptogenic processes is typically known, and hence, there is a window of opportunity during which the blockade of epileptogenesis may be possible.

For antiepileptogenesis target identification it is necessary to characterize the pathophysiological alterations that ultimately determine the

* Corresponding author.
** Corresponding author at: Sapienza University of Rome, Department of Physiology and Pharmacology, p.le Aldo Moro 5, 00185 Rome, Italy.
E-mail address: eleonora.palma@uniroma1.it (E. Palma).
[1] Shared last authorship

https://doi.org/10.1016/j.expneurol.2025.115183
Received 4 October 2024; Received in revised form 15 January 2025; Accepted 8 February 2025
Available online 10 February 2025

generation and recurrence of post-TBI acute and late seizures (Golub and Reddy, 2022). Based on previous data on models of status epilepticus (SE) and chronic seizures, dysfunction of GABAergic neurotransmission is one potential candidate pathomechanism (Brooks-Kayal and Russek, 2012; Grabenstatter et al., 2014). This scenario is frequently complicated by the aberrant expression of the cation-chloride cotransporters NKCC1 (Slc12a2) and KCC2 (Slc12a5), which is a hallmark of several epileptogenic pathologies (Alfano et al., 2022; Palma et al., 2006; Ruffolo et al., 2018). It leads to establishment of an immature inhibitory neurotransmission, due to altered chloride homeostasis, leading to depolarizing (or less hyperpolarizing) responses evoked by GABAergic activity (van Hugte et al., 2023). Furthermore, alterations in $GABA_A$ receptors ($GABA_ARs$) probably constitute one pathogenic factor contributing to the onset of epilepsy. However, they could also represent potential therapeutic targets since it is well known that a variation in the subunit composition of $GABA_ARs$ can mediate an increased or decreased sensitivity to pharmacological modulators, and that the modulation of chloride homeostasis *via* specific compounds (*e.g.,* Bumetanide) yielded promising results in preclinical studies on epilepsy models (Deidda et al., 2015; Tang et al., 2016).

Our objective was to identify key pathophysiological alteration of GABAergic activity which could be targeted to prevent or slow down epileptogenesis over the months after a TBI as well as mitigate early post-injury seizures. We used a well-characterized model of PTE induced with lateral fluid-percussion in rats, which recapitulates the occurrence of early and late seizures in human (Ndode-Ekane et al., 2024). First, we performed the molecular analysis of spatiotemporal expression of $GABA_AR$ subunits and genetic analysis of chloride transporters. Secondly, we studied the functional features of GABAergic transmission, taking advantage of the technique of membrane microtransplantation in *Xenopus* oocytes in order to overcome the technical difficulties that would stem from recording electrophysiological activity directly from highly damaged lesional and perilesional TBI brain tissues.

2. Materials and methods

Study design is summarized in Fig. 1.

2.1. Animals

Animals (33 sham-operated experimental controls, 84 TBI) were generated in four cohorts. ***Cohort 1*** consisted of 44 adult male Sprague–Dawley rats (Harlan Netherlands B.V., Horst, Netherlands) and was used for *in situ* hybridization (Drexel et al., 2015). Of these 10 were randomized into the sham-operated experimental control and 33 into the TBI group. ***Cohort 2*** included 29 adult male Sprague–Dawley rats (8 sham, 21 TBI; Harlan Netherlands B.V., Horst, Netherlands) and was used for immunohistochemistry (Drexel et al., 2015). ***Cohort 3*** included 10 adult male Sprague–Dawley rats (5 sham, 5 TBI; Harlan Netherlands B.V., Horst, Netherlands) and was used for mRNA-sequencing (mRNA-seq) followed by the GSEA analysis (Lipponen et al., 2016). ***Cohort 4*** consisted of 35 adult male Sprague–Dawley rats (10 sham, 25 TBI; Envigo B.V., Netherlands) and was used for electrophysiology when the amount of tissues was enough.

The rats were individually housed in a controlled environment (temperature 22 ± 1 °C; 50–60 % humidity; lights on from 07:00 to 19:00). Rats had free access to pellet food and water *ad libitum*. All animal procedures were approved by the Animal Ethics Committee of the Provincial Government of The Southern Finland and performed in accordance with the guidelines of the European Community Council Directives 2010/63/EU.

2.2. Induction of traumatic brain injury with lateral fluid-percussion -induced TBI

Traumatic brain injury (TBI) was induced using lateral fluid-percussion injury (FPI) as described in details previously (Kharatishvili et al., 2006; McIntosh et al., 1989). Briefly, animals were anesthetized and placed in a Kopf stereotactic frame (David Kopf Instruments, Tujunga, CA, USA) and the skull was exposed. Thereafter, a circular craniotomy (Ø 5 mm) was performed over the left parietal area midway between lambda and bregma, leaving the dura intact. Lateral FPI was induced after connecting the rat to a fluid-percussion device (AmScien Instruments, Richmond, VA, USA). The mean severity of the impact was 3.45 ± 0.01 atm in the *in situ* hybridization cohort, 3.38 ± 0.02 atm in the immunohistochemistry cohort, 3.32 ± 0.01 atm in the mRNA-seq cohort and 3.36 ± 0.01 atm in the electrophysiology cohort. Sham-operated experimental controls (n = 34) underwent all surgical procedures without the exposure to impact.

2.3. Nissl staining

Nissl staining was performed as described previously (Drexel et al., 2015). Sections were stained with Cresyl violet, dehydrated, cleared in butyl acetate, and coverslipped using *Eukitt* mounting medium (O. Kindler GmbH, Freiburg, Germany).

2.4. In situ hybridization

Tissue processing and the protocol for *in situ* hybridization is

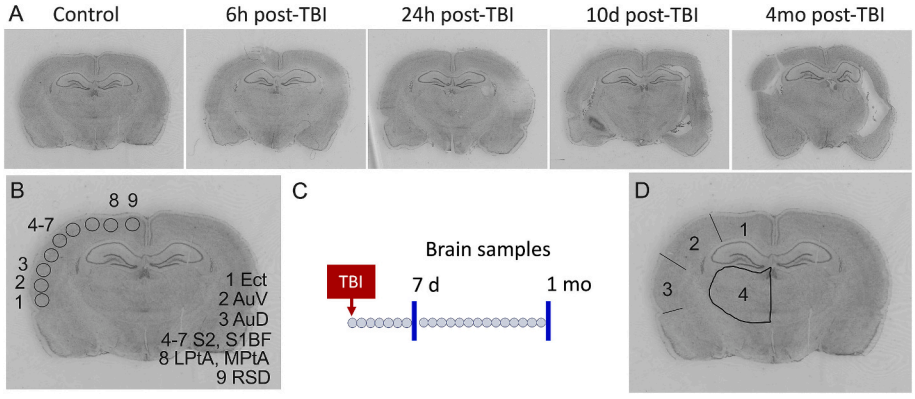

Fig. 1. *Study design and regions of interest (ROIs).* (A) Representative photomicrographs showing a section from a control rat and TBI rats at 6 h, 24 h, 10 d and 4 months after TBI. (B) Location of cortical ROIs used for *in situ* hybridization of $GABA_A$ receptor subunits. (C) Study design for the sampling of the brain tissue for electrophysiology. (D) ROIs sampled for electrophysiology. *Abbreviations*: AuD, dorsal auditory cortex; AuV, ventral auditory cortex; Ect, ectorhinal cortex; LPtA, lateral parietal association cortex; mo, months; MPtA, medial parietal association cortex; RSD, retrosplenial dysgranular cortex; S1BF, somatosensory barrel cortex; S2, secondary somatosensory cortex; TBI, traumatic brain injury.

described in detail previously (Drexel et al., 2015). Shortly, rats were sacrificed at 6 h, 24 h, 10 d or 4 months (6 animals per group) after TBI by cervical dislocation. The brains were dissected and snap-frozen by immersion into isopentane cooled to −70 °C. Brains from control animals were sampled at 24 h ($n = 5$) and 4 months ($n = 5$) after sham-injury and processed accordingly. Consecutive coronal 20-μm-thick sections were cut using a cryostat (Microm HM 560 M, Carl Zeiss AG, Vienna, Austria) at −20 °C, thaw-mounted on silane-coated slides and stored at −70 °C.

Sections from each rat sampled from the same rostro-caudal level (AP −3.30 to −4.15 from the bregma for all $GABA_A$ receptor subunits) were processed for *in situ* hybridization in the same incubation. The sequences of custom-synthesized oligonucleotides (Microsynth AG, Balgach, Switzerland) complementary to the respective mRNAs for $GABA_A$ receptor subunits (*Gabra1, Gabrg2, Gabrd* and *Gabrb3*) have been listed previously (Drexel et al., 2015; Tsunashima et al., 1997). *In situ* hybridization was performed as described previously (Tsunashima et al., 1997). The oligonucleotides (2.5 pmol) were labeled at the 3′-end with [^{35}S] α-thio-dATP (1300 Ci/mmol; New England Nuclear, Boston, MA, USA) by reaction with terminal deoxynucleotidyltransferase (Roche Austria GmbH, Vienna, Austria) and precipitated with 75 % ethanol and 0.4 % NaCl. Frozen sections (20 μm) were immersed in ice-cold paraformaldehyde (2 %) in phosphate-buffered saline (PBS), pH 7.2 for 10 min, rinsed in PBS, immersed in acetic anhydride (0.25 % in 0.1 mol/l triethylamine hydrochloride) at room temperature for 10 min, dehydrated by ethanol series, and delipidated with chloroform. The sections were then hybridized in 50 μl hybridization buffer containing about 50 fmol (0.8–1 × 10^6 cpm) labeled oligonucleotide probe for 18 h at 42 °C. The hybridization buffer consisted of 50 % formamide (Merck, Darmstadt, Germany), 2xSSC (1xSSC consisting of 150 mmol/l NaCl and 15 mmol/l sodium citrate, pH 7.2). The sections were then washed twice in 50 % formamide in 1xSSC (42 °C, 4 × 15 min), briefly rinsed in 1xSSC, rinsed in water, dipped in 70 % ethanol, dried, and then exposed to BioMax MR films (Sigma–Aldrich, Vienna, Austria) together with [^{14}C]-microscales (Amersham, Buckinghamshire, UK) for 14–28 d. Films were developed using Kodak D19 developer (Sigma–Aldrich, Vienna, Austria).

2.5. Densitometric analysis of messenger RNA expression

Autoradiographic films were digitized and analyzed using NIH ImageJ software (version 1.46; U.S. National Institutes of Health, Bethesda, ML, USA; http://imagej.nih.gov/ij/). For the analysis of $GABA_A$ receptor subunit intensities, ipsilateral cortex from the medial reference point to the rhinal fissure was divided to the nine regions of interest (ROIs) as described in Fig. 1. The mean gray value was measured for all these ROIs separately. Background staining was measured from the internal capsule in the same section (background region, 2.5 × 10^5 μm^2). The density of mean gray value of the $GABA_A$ receptor subunit was calculated by using the equation: (mean density of background ROI – density of mean gray value of the $GABA_A$ receptor subunit within a ROI)/mean density of background ROI. Representative digitized films of *in situ* hybridization signal for every subunit and time point are presented in a Supplementary Fig. 1.

2.6. Immunohistochemistry

Rats were perfused for immunohistochemistry at 6 h, 24 h, 10 d, or 4 months after TBI (four rats per group) as described previously (Drexel et al., 2015). Control animals were perfused at 24 h or 4 months (4 rats each time point) after sham-operation. Briefly, rats were deeply anesthetized and perfused through the ascending aorta with 50 ml PBS (50 mM phosphate buffer, pH 7.4, in 0.9 % NaCl) followed by 200 ml 4 % paraformaldehyde in PBS. Brains were immediately removed from the skull and postfixed in the same fixative for 90 min at 4–8 °C. Thereafter brains were cryoprotected in 20 % sucrose in 0.02 M PBS (pH 7.4) at 4–8 °C for 36 h and later rapidly frozen by immersion in −70 °C isopentane.

Immunohistochemistry for $GABA_A$ receptor subunits was done using free floating sections (30-μm-thick). Affinity purified antisera raised in rabbits against fusion proteins of peptide sequences (specific for the individual subunits) were used (Sperk et al., 1997). Goat anti-rabbit antibody coupled to horse radish peroxidase (P0448, Daco, Vienna) was used as secondary antibody (1:250) with subsequent labeling by reaction with 3,3-diaminobenzidine. Immunohistochemical staining of β2-sununit and δ-subunit were digitized and analyzed using NIH ImageJ software (version 1.46; U.S. National Institutes of Health, Bethesda, ML, USA; http://imagej.nih.gov/ij/). For the analysis of $GABA_A$ receptor subunit intensities, ipsilateral cortex from the medial reference point to the rhinal fissure was divided to the eleven regions of interest (ROIs) as described in (Hiltunen et al., 2021). The mean gray value was measured for all these ROIs separately (3–4 controls and 3–4 rats at 6 h or 24 h post-TBI). Background staining was measured from the internal capsule in the same section (background region, 2.5 × 10^5 μm^2). The density of mean gray value of the $GABA_A$ receptor subunit was calculated by using the equation: (mean density of background ROI – density of mean gray value of the $GABA_A$ receptor subunit within a ROI)/mean density of background ROI.

2.7. mRNA-seq and gene set enrichment analysis

Samples from the perilesional cortex and the ipsilateral thalamus were sequenced and analyzed as previously described (Lipponen et al., 2016). The raw data are available at the NCBI Gene Expression Omnibus (series accession number GSE80174; 5 controls and 5 TBI). For gene set enrichment analysis (GSEA), a pre-ranked gene list was created according to the mRNA sequencing dataset. The genes were arranged into negative and positive groups according to the fold-change values. Downregulated genes are identified with a minus sign. The genes were then arranged according to their *p*-value and ranked. Genes with high *p*-values were ranked closer to zero. The pre-ranked gene list created for gene enrichment analysis comprised 17,129 genes for the perilesional cortex and 18,562 genes for the ipsilateral thalamus. Human Gene Set for GABA receptor signaling was obtained from the MSigDB. (Subramanian et al., 2005) For the gene set used in the GSEA, BioMart (Smedley et al., 2009) was used to transcribe human gene symbols to corresponding rat ones.

2.8. Preparation of oocytes

Oocytes were obtained from adult *Xenopus laevis* females and treated as previously reported (Eusebi et al., 2009). The use of *Xenopus laevis* frogs, the surgical procedures for oocytes extraction and use conformed to the Italian Ministry of Health guidelines (authorization no 427/2020-PR) and were approved by the Local Committee for Animal Health (OPBA, Department of Physiology and Pharmacology, Sapienza University).

2.9. Membrane preparation

Using a Teflon glass homogenizer, about 0.5 g of previously frozen tissue was homogenized in 2 ml of glycine buffer (200 mM glycine/150 mM NaCl/50 mM EGTA/50 mM EDTA/300 mM sucrose), plus 20 μl of protease inhibitors (Sigma P2714), pH 9 with NaOH. The filtrate was centrifuged for 15 min at 9.500 ×*g* in a Beckmann centrifuge (C1015 rotor). The supernatant was then centrifuged for 2 h at 100.000 ×g in a SW40 rotor at 4 °C in a Beckmann centrifuge. The pellet was washed, resuspended in 5 mM glycine, aliquoted and stored at −80 °C (Miledi et al., 2002).

The day after the removal, the oocytes were injected with experimental sample using a manual microinjection system (Drummond Scientific Company, Broomall, PA). Injected volume was 80 nl/oocyte of

cortical and thalamic membranes from TBI and control rats. The oocytes were ready for current recording 24 h after injection.

2.10. Electrophysiology

Electrophysiological studies were performed using the Two-Electrode Voltage Clamp (TEVC) technique. Borosilicate microelectrodes, with a tip resistance of 0.5–4 MΩ, were filled with 3 M KCl. Oocytes were continuously performed by the external solution Oocyte Ringer solution (OR in mM: NaCl 82.5; KCl 2.5; $CaCl_2$ 2.5; $MgCl_2$ 1; Hepes 5, adjusted to pH 7.4 with NaOH).

Current responses were evoked perfusing the oocytes with 500 μM GABA. Unless otherwise stated the recordings were performed at a holding potential (V_H) of −60 mV. When constructing current-voltage (I-V) relationships the V_H was stepped for 2–4 min at the desired value before applying the neurotransmitter. For these experiments, electrodes were filled with K-Acetate (3 M – (Conti et al., 2011) to reduce the leakage of high concentration of Cl- from electrodes into the oocytes. However, the experiments gave same results when KCl filling solution was used (not shown). The GABA reversal potential (E_{GABA}) was determined by fitting the I-V relationships with a regression curve-fitting software (Sigmaplot 12 software). Data analysis was performed using Clampfit 10.2 software (Molecular Devices, Sunnyvale, CA, United States, www.moleculardevices.com); OriginPro 8.0 (OriginLab Corp., Northampton, MA, United States, www.originlab.com).

2.11. Statistical analysis

Data was analyzed by using IBM SPSS Statistics 23 for Windows. Differences in intensities between the groups were analyzed using the Kruskal-Wallis test. *Post hoc* analysis was performed using the Mann-Whitney *U* test. Differences in the protein levels were assessed using Mann-Whitney *U* test. Mortality between the cohorts was tested using GraphPad Prism 10 and Fisher's exact test. Sigmaplot 15 software (Systat software Inc., Chicago, IL, USA) was used for statistical analysis for electrophysiological studies. We assessed normal distribution with the Shapiro–Wilk test in order to choose parametric (Student's *t*-test) or non-parametric (Wilcoxon signed rank test, Mann–Whitney rank sum test) tests before starting the data analysis process. A p-value <0.05 was considered significant. CorelDraw X10 software was used for figure preparation.

3. Results

3.1. Mortality

The acute post-injury mortality during first 48 h after TBI was 27 % (9/33) in the *in situ* hybridization cohort, 24 % (5/21) in the immunohistochemistry cohort, 17 % (3/18, (Lipponen et al., 2016); 5 TBI animals included to this study) in the mRNA-seq sequencing and GSEA cohort and 20 % (5/25) in the electrophysiology cohort ($p > 0.05$ between the cohorts). In the electrophysiology cohort the average duration

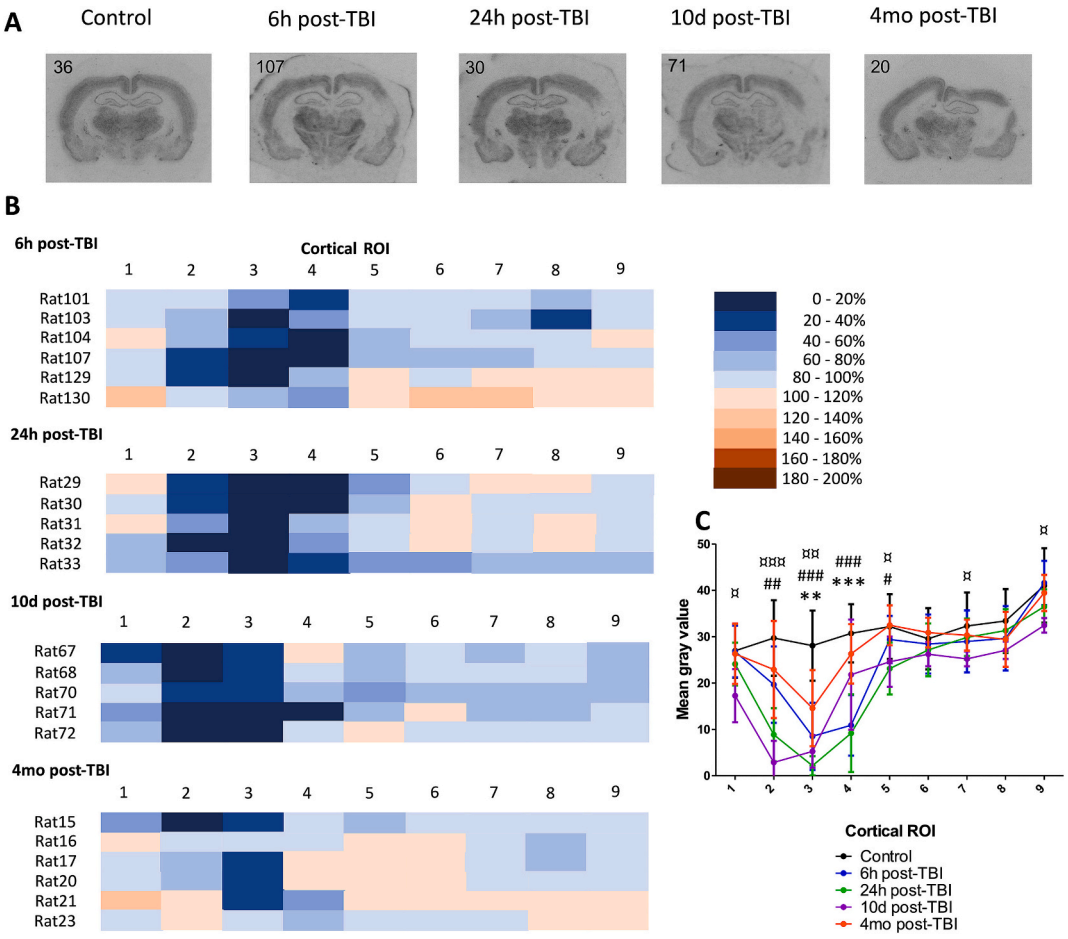

Fig. 2. *In situ* hybridization of α1-subunit of $GABA_A$ receptor in the perilesional cortex. (A) Representative digitized films of *in situ* hybridization signal of the α1-subunit in a control rat (left panel) and in TBI rats at different post-TBI timepoints (6 h, 24 h, 10 d and 4 months). (B) Heatmaps demonstrating the average %-changes in the mRNA signal intensity of the 9 ROIs (see Fig. 1B) in rats with TBI as compared to sham-operated controls. (C) Evolution of *in situ* hybridization signal changes (y-axis) in different ROIs (x-axis, see Fig. 1B). *Abbreviations*: ROI, region of interest; TBI, traumatic brain injury. *Statistical significances*: **, $p < 0.01$; ***, $p < 0.001$ at 6 h post-TBI; ##, $p < 0.01$, ###, $p < 0.001$at 24 h post-TBI; ¤, $p < 0.05$; ¤¤, $p < 0.01$, ¤¤¤, $p < 0.01$ at 10 d post-TBI.

of the post-impact apnea was 29 s (range 15–50 s). Nissl staining depicted the typical cortical and thalamic injuries (Fig. 1A). For other cohorts, details of the injury parameters have been reported previously (Drexel et al., 2015; Lipponen et al., 2016).

3.2. Transient downregulation of α1-subunit in the perilesional cortex

To estimate gene-expression change of the α1-subunit, the mean gray values of the mRNA *in situ* hybridization signal in and around the perilesional cortex were measured at 6 h, 24 h, 10 d and 4 months post-TBI and compared to controls (Fig. 2A). Already at 6 h post-TBI, the loss of α1-subunit was evident in the dorsal auditory (AuD; ROI 3, $p < 0.01$, Fig. 2B-C) and somatosensory cortex (ROI 4, $p < 0.001$, Fig. 2B- C) and at 24 h post-TBI it was extended more to the ventral auditory cortex (AuV) direction (ROI 2, $p < 0.01$; ROI 3, $p < 0.001$; ROI 4, $p < 0.001$, Fig. 2B-C). The loss of α1-subunit was most pronounced at 10d post-TBI, as it extended through all measured areas (ROI 1, $p < 0.05$; ROI 2, $p < 0.001$; ROI 3, $p < 0.01$; ROI 5, $p < 0.05$; ROI 7, $p < 0.05$; ROI 9, $p < 0.05$; Fig. 2B-C), except part of the somatosensory cortex (ROI 4 and ROI 6; Fig. 2B-C) and lateral parietal association cortex (LPtA, ROI 8; Fig. 2B-C). No difference in the gene expression was observed at 4 months post-TBI. When the protein labeling of the α1-subunit was estimated from immunohistochemical staining, no difference in any time point was found in our qualitative analysis (Supplementary Fig. 2).

3.3. Downregulation of β2-subunit in the perilesional cortex

To estimate gene-expression change of the β2-subunit, the mean gray values of the mRNA *in situ* hybridization signal in and around the perilesional cortex were measured at 6 h, 24 h, 10 d and 4 months post-TBI were compared to controls (Fig. 3A). At 6 h post-TBI, downregulation was observed in the AuD (ROI 3, $p < 0.01$, Fig. 3B-C) and somatosensory areas S1 and S2 (ROI 4, $p < 0.01$, Fig. 3B-C). A more widespread downregulation was seen at 24 h post-TBI as TBI rats had decreased β2-subunit in AuV (ROI 2, $p < 0.01$, Fig. 3B-C), in AuD (ROI 3, $p < 0.01$, Fig. 3B-C) and in S1 and S2 (ROI 4, $p < 0.01$, ROI 5, $p < 0.05$, Fig. 3B-C). Gene expression recovery close to control levels was observed at 10 d post-TBI. However, there was still a downregulation of β2-subunit in AuV (ROI 2, $p < 0.01$, Fig. 3B-C) as well as in AuD (ROI 3, $p < 0.01$, Fig. 3B-C). At 4 months post-TBI downregulation of β2-subunit was still present in AuD (ROI 3, $p < 0.05$, Fig. 3B-C). In addition, we observed a slight increase in β2-subunit level at retrosplenial dysgranular cortex (RSD; ROI 9, $p < 0.05$, Fig. 3B-C). Protein levels of β2-subunit followed the levels of mRNA in our qualitative analysis (Supplementary Fig. 2). A trend towards quantitative down-regulation was observed within the auditory areas (ROI 3–5; $p > 0.05$; Supplementary Fig. 3).

3.4. Dysregulation of β3-subunit in the perilesional cortex

To estimate gene-expression change of the β3-subunit, the mean gray values of the mRNA *in situ* hybridization signal in and around the

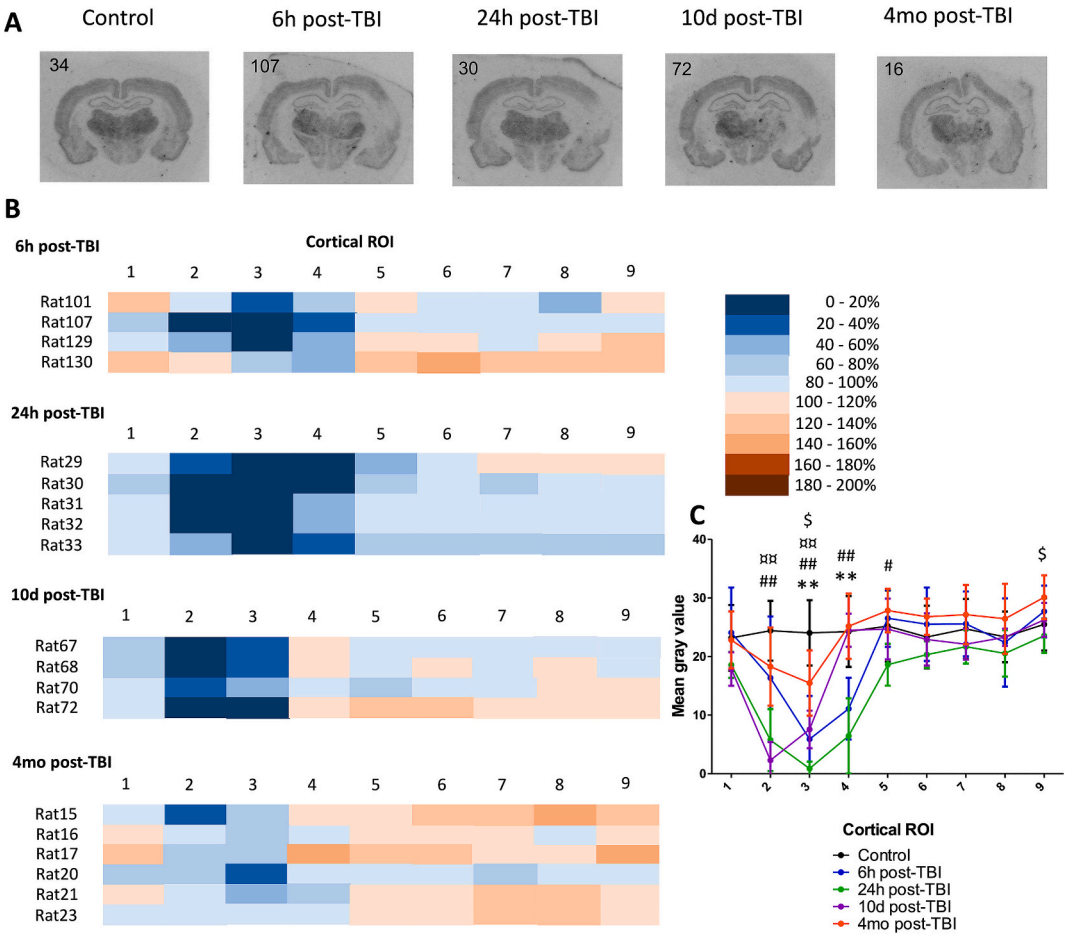

Fig. 3. *In situ hybridization of β2-subunit of $GABA_A$ receptor in the perilesional cortex.* (A) Representative digitized films of *in situ* hybridization signal of the β2-subunit in a control rat (left panel) and in rats with TBI at different post-TBI timepoints (6 h, 24 h, 10 d and 4 months). (B) Heatmaps demonstrating the average %-changes in the mRNA signal intensity of the 9 ROIs (see Fig. 1B) in TBI rats as compared to sham-operated controls. (C) Evolution of *in situ* hybridization signal changes (y-axis) in different ROIs (x-axis, see Fig. 1B). *Abbreviations*: ROI, region of interest; TBI, traumatic brain injury. *Statistical significances*: **, $p < 0.01$ at 6 h post-TBI; #, $p < 0.05$, ##, $p < 0.01$ at 24 h post-TBI; ¤¤, $p < 0.01$ at 10 d post-TBI; $, $p < 0.05$ at 4 months post-TBI.

perilesional cortex were measured at 6 h, 24 h, 10 d and 4 months post-TBI were compared to that in controls (Fig. 4A). At 6 h post-TBI we observed a downregulation of β3-subunit in AuD (ROI 3, $p < 0.01$, Fig. 4B-C) as well as in S1-S2 (ROI 4, $p < 0.05$, Fig. 4B-C). At this time point slight upregulation of β3-subunit was seen in Ect (ROI 1, $p < 0.05$, Fig. 4B-C), somatosensory cortex (ROI 6, $p < 0.05$, Fig. 4B-C) and RSD (ROI 9, $p < 0.05$, Fig. 4B-C). This upregulation faded away by 24 h post-TBI as at that time point downregulation of β3-subunit was present only in AuV (ROI 2, $p < 0.01$, Fig. 4B-C), AuD (ROI 3, $p < 0.01$, Fig. 4B-C) and S1-S2 (ROI 4, $p < 0.01$, Fig. 4B-C). Expression profile of β3-subunit followed previously seen (other subunits) pattern at 10 d post-TBI as downregulation was present in AuV (ROI 2, $p < 0.001$, Fig. 4B-C) and AuD (ROI 3, $p < 0.001$, Fig. 4B-C). Interestingly, at 4 months post-TBI, there was a robust increase in the β3-subunit gene expression outside the evident lesion core. Upregulation was present in Ect (ROI 1, $p < 0.01$, Fig. 4B-C), S1-S2 (ROI 4, $p < 0.01$, ROI 5, $p < 0.001$, ROI 6, $p < 0.001$, ROI 7, $p < 0.001$; Fig. 4B-C), LPtA/ MPtA (ROI 8, $p < 0.01$, Fig. 4B-C) and RSD (ROI 9, $p < 0.001$, Fig. 4B-C). Downregulation of protein levels were observed at 6 h, 24 h and 10 d post-TBI (Supplementary Fig. 2). However, no clear upregulated profile of β3-subunit was found at 4 months post-TBI at protein level.

3.5. Dysregulation of γ2-subunit in the perilesional cortex

To estimate gene-expression change of the γ2-subunit, the mean gray values of the mRNA *in situ* hybridization signal in and around the perilesional cortex were measured at 6 h, 24 h, 10 d and 4 months post-TBI were compared to controls (Fig. 5A). Downregulation of γ2-subunit was found in the in AuD (ROI 3, $p < 0.05$, Fig. 5B-C) as well in S1-S2 (ROI 4, $p < 0.05$, Fig. 5B-C) and upregulation in part of the somatosensory cortex (ROI 6, $p < 0.05$, Fig. 5B-C) and in RSD (ROI 9, $p < 0.01$, Fig. 5B-C) at 6 h post-TBI. At 24 h post-TBI, downregulation of γ2-subunit was seen in the AuV (ROI 2, $p < 0.01$, Fig. 5B-C), AuD (ROI 3, $p < 0.01$, Fig. 5B-C and S1-S2 (ROI 4, $p < 0.01$, Fig. 5B-C). In addition, we observed an upregulation of γ2-subunit in the part of the somatosensory cortex (ROI 6, $p < 0.01$, Fig. 5B-C). Expression profile of γ2-subunit followed previously seen (other subunits) pattern at 10 d post-TBI as downregulation was present in AuV (ROI 2, $p < 0.01$, Fig. 5B-C) and AuD (ROI 3, $p < 0.01$, Fig. 5B-C). As compared to other subunits, limited changes in γ2-subunit gene expression were observed at 4 months post-TBI; we showed only a downregulation of γ2-subunit in the AuD (ROI 3, $p < 0.05$, Fig. 5B-C) and upregulation in part of the somatosensory cortex (ROI 6, $p < 0.05$, Fig. 5B-C). Protein levels were following the levels of the mRNA in all time points (Supplementary Fig. 2).

3.6. Dysregulation of δ-subunit in the perilesional cortex

To estimate gene-expression change of the δ-subunit, the mean gray values of the mRNA *in situ* hybridization signal in and around the perilesional cortex were measured at 6 h, 24 h, 10 d and 4 months post-TBI were compared to that in controls (Fig. 6A). At 6 h post-TBI, similar to β3-subunit, we found a downregulation of δ-subunit in AuD (ROI 3, $p <$

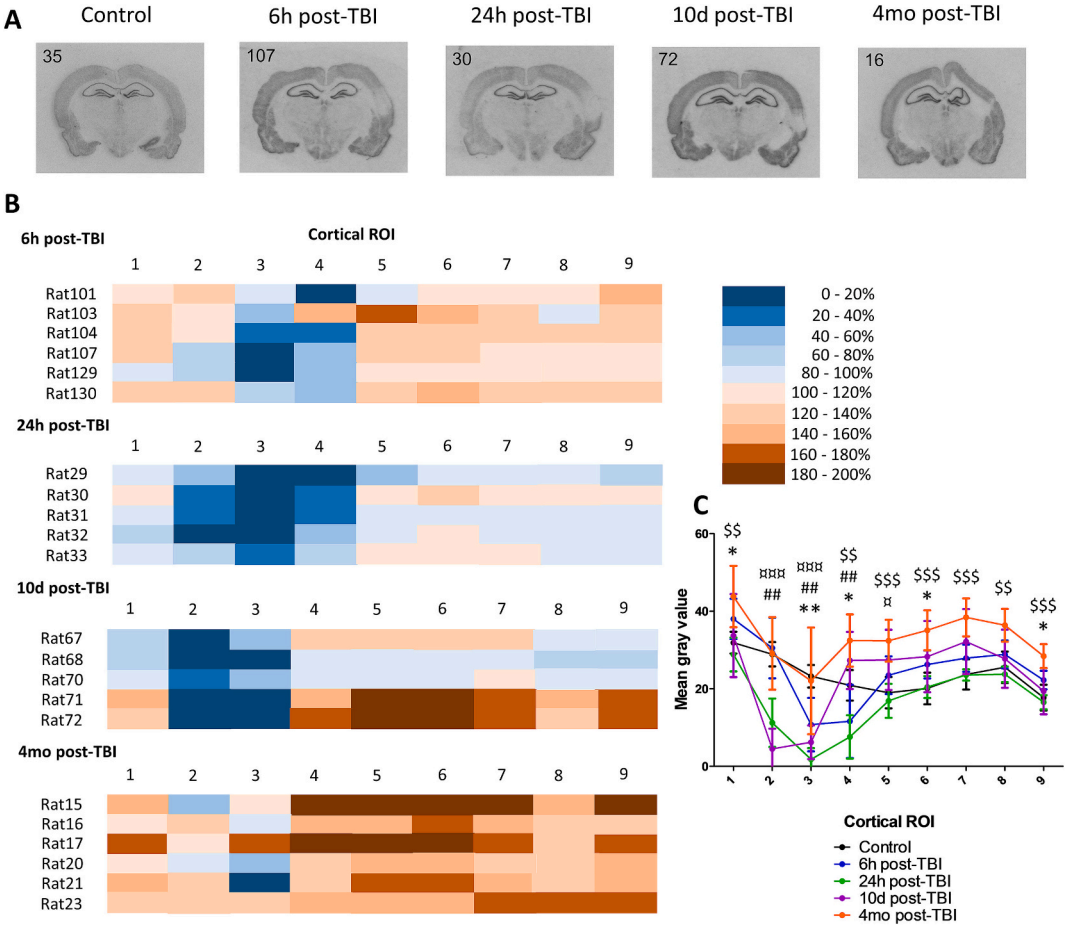

Fig. 4. *In situ hybridization of β3-subunit of $GABA_A$ receptor in the perilesional cortex.* (A) Representative digitized films of *in situ* hybridization signal of the β3-subunit in a control rat (left panel) and in rats with TBI at different post-TBI timepoints (6 h, 24 h, 10 d and 4 months). (B) Heatmaps demonstrating the average %-changes in the mRNA signal intensity of the 9 ROIs (see Fig. 1B) in TBI rats as compared to sham-operated controls. (C) Evolution of *in situ* hybridization signal changes (y-axis) in different ROIs (x-axis, see Fig. 1B). *Abbreviations*: ROI, region of interest; TBI, traumatic brain injury. *Statistical significances*: *, $p < 0.05$, **, $p < 0.01$ at 6 h post-TBI; ##, $p < 0.01$ at 24 h post-TBI; ¤¤¤, $p < 0.001$ at 10 d post-TBI; $$, $p < 0.01$; $$$, $p < 0.001$ at 4 months post-TBI.

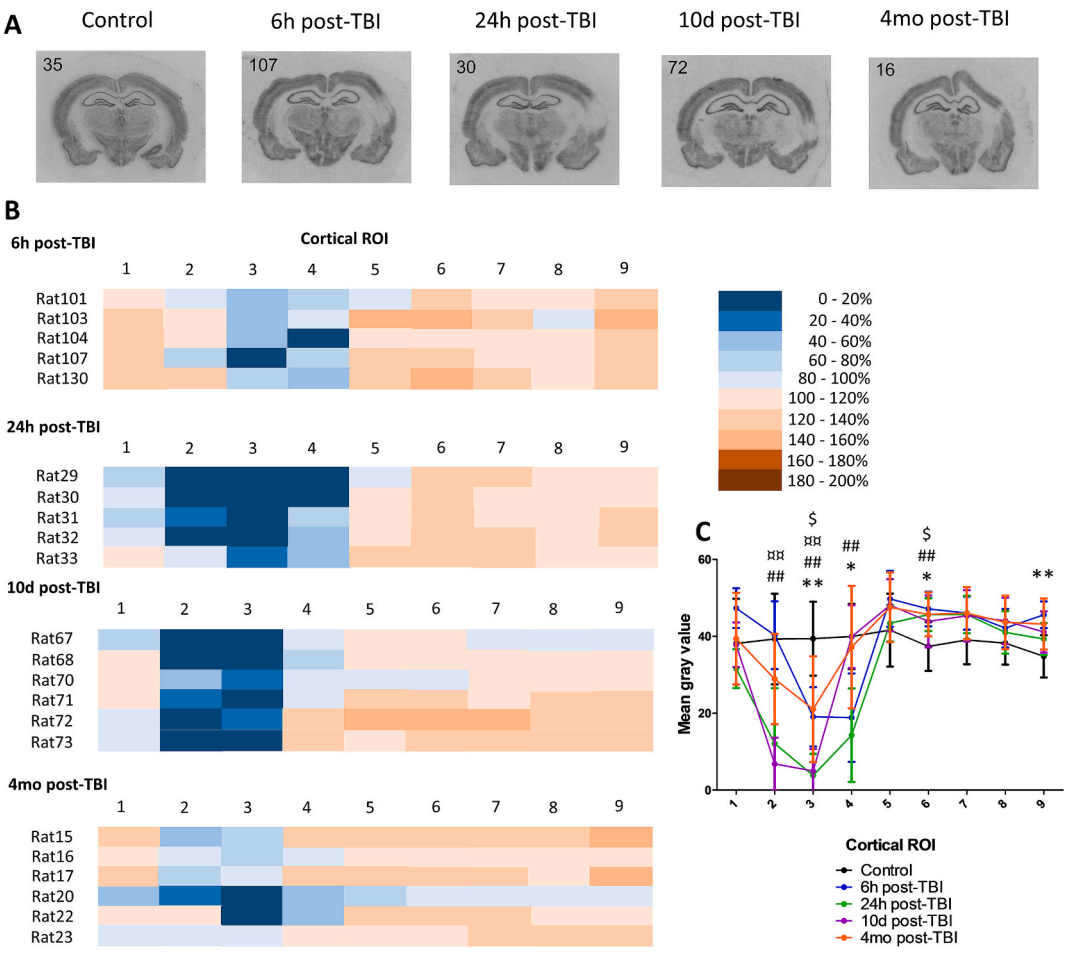

Fig. 5. *In situ hybridization of the γ2-subunit of $GABA_A$ receptor in the perilesional cortex.* (A) Representative digitized films of *in situ* hybridization signal of the γ2-subunit in a control rat (left panel) and in rats with TBI at different post-TBI timepoints (6 h, 24 h, 10 d and 4 months). (B) Heatmaps demonstrating the average %-changes in the mRNA signal intensity of the 9 ROIs (see Fig. 1B) in TBI rats as compared to sham-operated controls. (C) Evolution of *in situ* hybridization signal changes (y-axis) in different ROIs (x-axis, see Fig. 1B). *Abbreviations*: ROI, region of interest; TBI, traumatic brain injury. *Statistical significances*: *, $p < 0.05$, **, $p < 0.01$ at 6 h post-TBI; ##, $p < 0.01$ at 24 h post-TBI; ¤¤, $p < 0.01$ at 10 d post-TBI; $, $p < 0.05$ at 4 months post-TBI.

0.05, Fig. 6B-C) as well as in S1-S2 (ROI 4, $p < 0.05$; Fig. 6B-C). Further, an upregulation was seen in the part of the somatosensory cortex (ROI 6, $p < 0.05$, ROI 7, $p < 0.01$; Fig. 6B-C), LPtA/MPtA (ROI 8, $p < 0.01$, Fig. 6B-C) and RSD (ROI 9, $p < 0.05$, Fig. 6B-C). At 24 h post-TBI, a robust downregulation of δ-subunit was present in the perilesional cortex. Specifically, it was seen in the Ect (ROI 1, $p < 0.01$, Fig. 6B-C), AuV (ROI 2, $p < 0.01$, Fig. 6B-C), AuD (ROI 3, $p < 0.01$, Fig. 6B-C) and S1-S2 (ROI 4, $p < 0.01$, Fig. 6B-C). In addition, we observed a slight downregulation of δ-subunit in RSD (ROI 9, $p < 0.05$, Fig. 6B-C). Expression profile of δ-subunit at 10 d post-TBI was comparable to that of the other subunits, showing a downregulation in AuV (ROI 2, $p < 0.01$, Fig. 6B-C) and AuD (ROI 3, $p < 0.01$, Fig. 6B-C). At 4 months post-TBI, there was a robust increase in δ-subunit gene expression outside the lesion core, similar to that seen for β3-subunit. Upregulation was present in Ect (ROI 1, $p < 0.05$, Fig. 6B-C), S1-S2 (ROI 4, $p < 0.01$, ROI 5, $p < 0.01$, ROI 6, $p < 0.01$, ROI 7, $p < 0.01$; Fig. 6B-C), LPtA/ MPtA (ROI 8, $p < 0.01$, Fig. 6B-C) and RSD (ROI 9, $p < 0.01$, Fig. 6B-C). Protein levels of δ-subunit were in correlation with the quantitative mRNA analysis (Supplementary Fig. 1). A mild downregulated trend of δ-subunit was observed at acute time points post-TBI, but only in the deep layers ($p > 0.05$, $n = 4$; Supplementary Fig. 3).

3.7. Molecular profiling of GABA signaling post-TBI

To further profile GABA signaling at a more chronic time point (3 months post-TBI) we analyzed the mRNA-seq dataset available using GSEA (Lipponen et al., 2016). Interestingly, in the perilesional cortex we found a robust negative enrichment of GABA signaling (ES = -0.62, $p = 0.0$; Fig. 7A). Among the most downregulated genes were *Gabrg2*, *Slc32a1*, *Gabbr2*, *Gabrd* and *Gad1*. A negative enrichment of GABA signaling was also found in the ipsilateral thalamus (ES = -0.44, $p < 0.01$; Fig. 7B). Among the most downregulated genes were *Gabrb2*, *Gabra1*, *Gabra4*, Slc6a1 and *Gabrd*.

Since it is well-established that the chloride homeostasis can be altered in different epilepsies, (Braat and Kooy, 2015) we also analyzed the dysregulation of *Slc12a5* and *Slc12a2* genes, encoding the chloride-transporter proteins *KCC2* and *NKCC1*, respectively. In the perilesional cortex, *Slc12a5* was downregulated ($\log2FC = -0.47$, $p < 0.001$, Fig. 7C) while the gene expression of *Slc12a2* showed just a mild non-significant trend towards upregulation ($\log2FC = 0.25$, $p > 0.05$, Fig. 7A). Like in the perilesional cortex, also in the ipsilateral thalamus, *Slc12a5* was downregulated ($\log2FC = -0.42$, $p < 0.05$, Fig. 7C). However, *Slc12a2* gene expression was upregulated ($\log2FC = 0.50$, $p < 0.05$, Fig. 7D).

3.8. Functional features of GABA currents post-TBI

Next, we assessed whether regulated chloride transporters expression can alter the functional properties of $GABA_AR$, using micro-transplantation of perilesional brain or thalamic membranes from post-

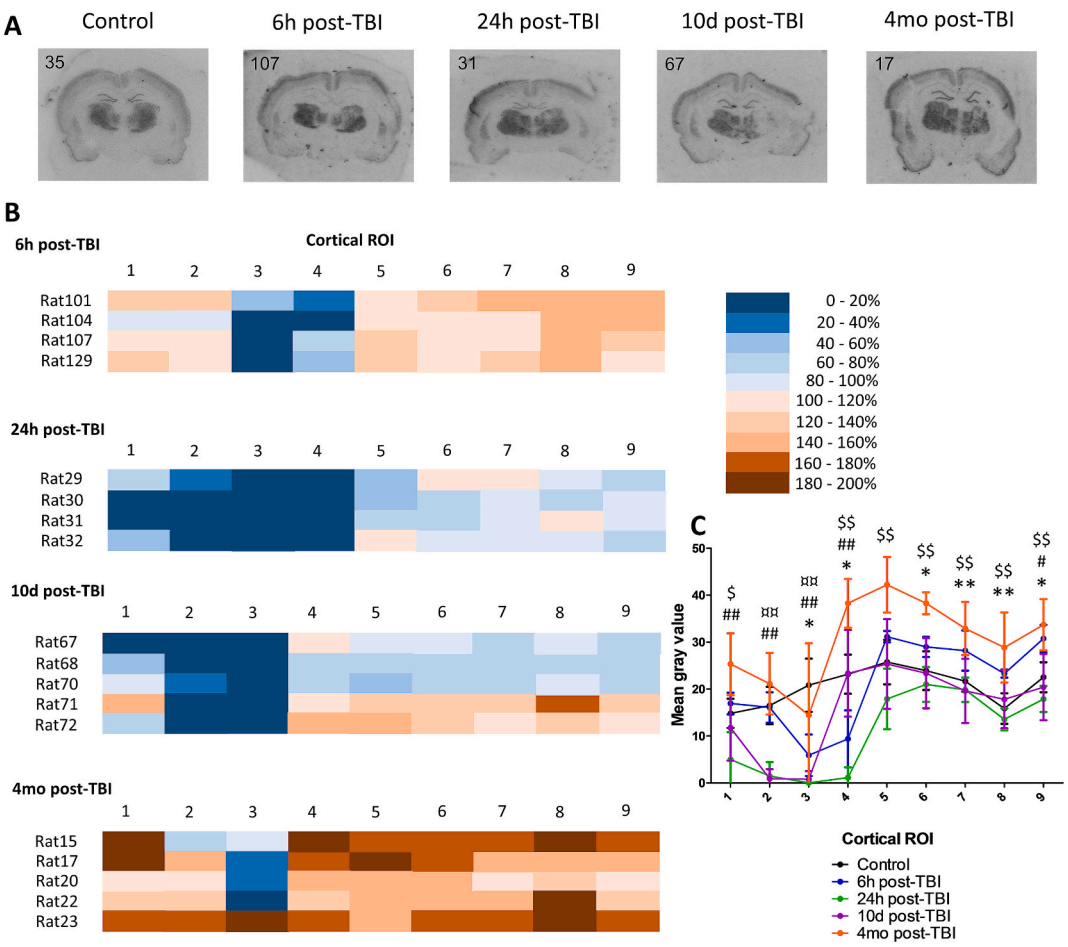

Fig. 6. *In situ hybridization of the δ-subunit of GABA$_A$ receptor in the perilesional cortex*. (A) Representative digitized films of *in situ* hybridization signal of the δ-subunit in a control rat (left panel) and in rats with TBI at different post-TBI timepoints (6 h, 24 h, 10 d and 4 months). (B) Heatmaps demonstrating the average %-changes in the mRNA signal intensity of the 9 ROIs (see Fig. 1B) in TBI rats as compared to sham-operated controls. (C) Evolution of *in situ* hybridization signal changes (y-axis) in different ROIs (x-axis, see Fig. 1B). *Abbreviations*: ROI, region of interest; TBI, traumatic brain injury. *Statistical significances*: *, $p < 0.05$, **, $p < 0.01$ at 6 h post-TBI; #, $p < 0.05$, ##, $p < 0.01$ at 24 h post-TBI; ¤¤, $p < 0.01$ at 10 d post-TBI; $, $p < 0.05$; $$, $p < 0.01$ at 4 months post-TBI.

TBI rats to *Xenopus* oocytes at 1-month post-injury or sham-operation. The time point was selected as it is clearly beyond the occurrence of the early seizures, but before the onset of late unprovoked seizures (Andrade et al., 2018; Kharatishvili et al., 2006). The approach allowed the measurements of GABA-evoked currents (I_{GABA}), while maintaining the native characteristics of $GABA_A$ receptors (Palma et al., 2003). Firstly, we tried to record GABA-evoked currents from lesional area (ROI 3, Fig. 1D) but, as expected, we could not record any functional responses due to the severe damage that characterizes the lesion core. Subsequently, we investigated the GABA reversal potential (E_{GABA}) in different perilesional cortical areas (ROI 1 and 2, Fig. 1D, Fig. 8) and thalamus (ROI 4, Fig. 1D, Fig. 9) both ipsilaterally and contralaterally.

Application of GABA (500 μM) was able to elicit genuine, bicuculline sensitive I_{GABA} (not shown) with amplitude values ranging from 30 to 220 nA (121.5 ± 25.5, 12 rats, $n = 105$).

3.8.1. Cortex

In sham-operated experimental controls, E_{GABA} values did not differ between ipsilateral and contralateral ROIs (both ROI 1 and 2) in any of the areas tested (ROI 1 ipsilateral, E_{GABA}: −27.0 ± 1.5 mV, 2 rats, $n = 20$ *vs.* ROI 1 contralateral, E_{GABA}: −25.6 ± 2.0 mV, 2 rats, n = 20; ROI 2 ipsilateral, $_{GABA}$: −26.7 ± 1.7 mV, 2 rats, $n = 18$ *vs.* ROI 2 contralateral, E_{GABA}: −26.3 ± 1.8 mV, 2 rats, $n = 22$; Fig. 8C).

In cortical ROI 1 of the rats with TBI, we found a more depolarized E_{GABA} in oocytes transplanted with membranes from ipsilateral (E_{GABA} = −20.6 ± 4.3 mV, 4 rats, $n = 28$) than contralateral side (E_{GABA} = −26.3 ± 1.7 mV, 4 rats, $n = 26$; $p < 0.05$), Fig. 8A, B). Furthermore, the E_{GABA} value found in ipsilateral TBI ROI 1 was statistically different from that previously recorded in sham animals ($p < 0.05$). In ROI 2, that was adjacent to ROI 1 towards midline, E_{GABA} values aligned with those in ROI 1, being less hyperpolarized ipsilaterally (E_{GABA}: −20.3 ± 2.9 mV, 2 rats, $n = 21$) than contralaterally (E_{GABA}: −26.6 ± 2.7 mV, 2 rats, n = 20; $p < 0.05$). Again, the altered E_{GABA} value found in ipsilateral TBI ROI 2 was clearly different from that previously recorded in sham animals ($p < 0.05$). These findings indicate a clear shift of E_{GABA} towards more depolarized values in the ipsilateral than contralateral perilesional cortex. In addition, we performed further experiments using the selective NKCC1 blocker Bumetanide (12 μM for two hours, (Ruffolo et al., 2016). Notably, Bumetanide was able to shift the depolarized E_{GABA} values in the ipsilateral ROI 1 of TBI-rats (−22 ± 0.7 mV, before and −27.4 ± 0.5, after Bumetanide; n = 10, $p < 0.001$, paired *t*-test). In contrast, as expected, E_{GABA} values in the contralateral ROI 1 of TBI-rats was unaffected by Bumetanide treatment (−27.9 ± 1.8 mV, before and − 28.5 ± 0.6 mV, after Bumetanide; $n = 8$, $p > 0.05$, paired t-test, Supplementary Fig. 4). The interhemispheric difference in E_{GABA} after TBI was not related to a difference in evoked GABA currents (ipsilateral I_{GABA}: −35.8 ± 7.1 nA, 8 rats, $n = 49$ *vs.* contralateral I_{GABA}: −27.6 ± 5.0 nA, 8 rats, $n = 46$, V_H = -60 mV, $p > 0.05$).

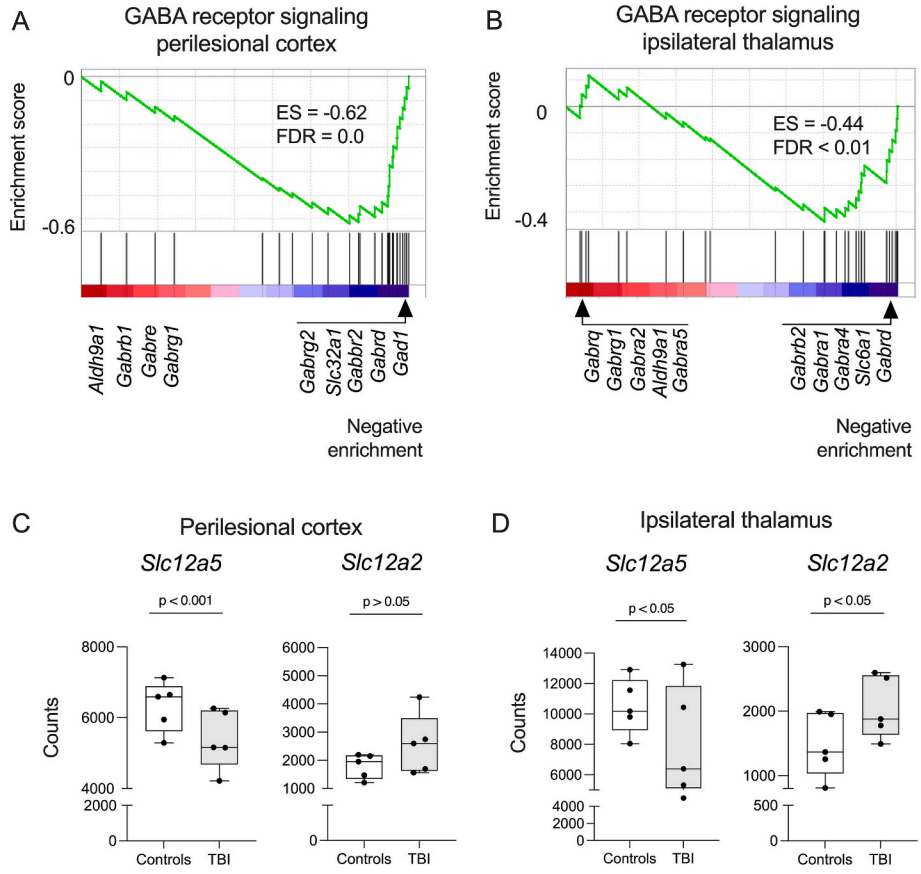

Fig. 7. *Molecular profiling of GABA signaling at 3 months post-TBI.* (A) A robust negative enrichment of GABA signaling was observed in the perilesional cortex at 3 months post-TBI as compared to controls with GSEA (ES = -0.62, $p = 0.0$). Among the most downregulated genes were *Gabrg2*, *Slc32a1*, *Gabbr2*, *Gabrd* and *Gad1*. (B) A negative enrichment of GABA signaling was observed also in the ipsilateral thalamus (ES = -0.44, $p < 0.01$). Among the most downregulated genes were *Gabrb2*, *Gabra1*, *Gabra4*, Slc6a1 and *Gabrd*. (C) In the perilesional cortex, *Slc12a5* (log2FC = −0.47, $p < 0.001$,) was downregulated while the gene expression of *Slc12a2* remained unchanged (log2FC = 0.25, $p > 0.05$). (D) Also, in the ipsilateral thalamus, *Slc12a5* (log2FC = −0.42, $p < 0.05$) was downregulated while the gene expression of *Slc12a2* was upregulated (log2FC = 0.50, $p < 0.05$). *Abbreviations*: ES, enrichment score; FDR, false discovery rate; *Slc12a2,* Solute Carrier Family 12 Member 2; *Slc12a5*, Solute Carrier Family 12 Member 5, TBI, traumatic brain injury.

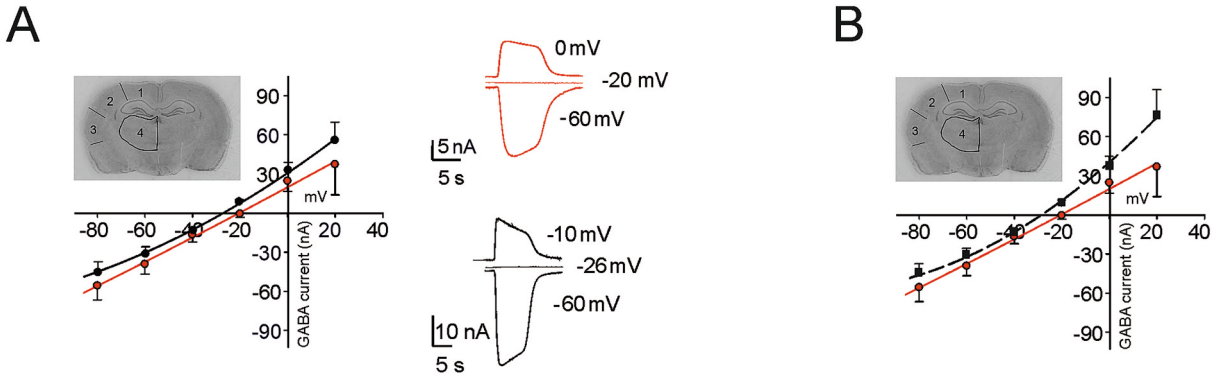

Fig. 8. *Alterations in GABA current reversal potential (E_{GABA}) in the perilesional cortex after TBI.* Current-voltage (I-V) relationships obtained from: (A) oocytes injected with membranes from the ipsilateral ($n = 28$; ROI 1, ●) and contralateral cortex ($n = 26$; ROI 1, ●) of TBI-rats; (B) oocytes injected with membranes from the ipsilateral cortex (n = 28; ROI 1, ●) of TBI-rats and ipsilateral cortex ($n = 20$; ROI 1, ■) of sham-rats. The points represent mean ± SEM of the current (nA) evoked at each holding potential (V_H). *Inset* shows the areas of different ROIs. The rightward *insets* in (A) show sample currents from the same experiments at different V_H (mV) in ipsilateral (red traces) and contralateral cortex (black traces) of TBI-rats. (For interpretation of the references to colour in this figure legend, the reader is referred to the web version of this article.)

3.8.2. *Thalamus*

In sham animals, E_{GABA} values showed no interhemispheric difference (ROI 4 ipsilateral E_{GABA} -24.3 ± 1.9 mV, 2 rats, $n = 12$ *vs.* ROI 4 contralateral E_{GABA} -24.13 ± 1.2 mV, 2 rats, n = 10, *not shown*). In the thalamic ROI 4 of rats with TBI, abnormalities in E_{GABA} were similar to that found in the perilesional cortex, being more depolarized ipsilaterally (E_{GABA} -19.8 ± 0.85 mV, 4 rats, $n = 25$) than contralaterally (E_{GABA} -24.4 ± 0.6 mV, 4 rats, n = 25; $p < 0.05$; Fig. 9). Again, the E_{GABA} value

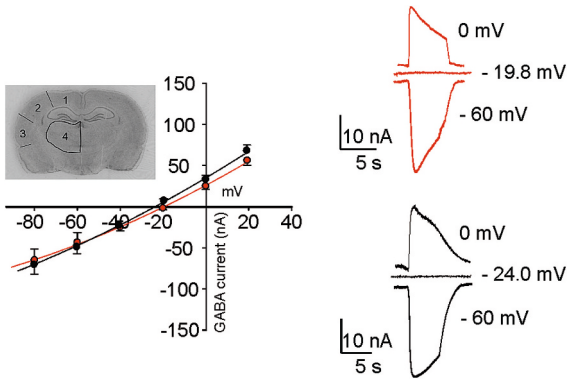

Fig. 9. *Alteration of GABA currents reversal potential (E_{GABA}) in the thalamus after TBI.* Current-voltage (I-V) relationships obtained from oocytes injected with perilesional membranes from the ipsilateral (●) and contralateral (●) thalamus (ROI 4, $n = 25$ for each sample). The points show the mean ± SEM of the current (nA) evoked at each holding potential (V_H). The *insets* show sample currents from the same experiments at different V_H (mV).

found in ipsilateral TBI thalamus was statistically different from that previously recorded in sham animals ($p < 0.05$). As in the cortex, the evoked GABA currents showed no interhemispheric difference (ipsilateral I_{GABA} − 43.5 ± 11 nA, n = 25 *vs.* contralateral I_{GABA} -48.2 ± 8.0 nA; n = 25, VH = -60 mV). In additional experiments we used Zn^{2+} to block the extrasynaptic component of the $GABA_A$-Rs. Interestingly using 40 μM Zn^{2+} co-applied with 200 μM GABA (Palma et al., 2007), we did not find any statistical difference between ipsilateral and contralateral of TBI rats (residual GABA currents as percentage of control currents: ipsilateral 71.7 ± 2.4 % *vs* contralateral 79 0.7 ± 3.1 %; n = 8; p = 0.072, paired t-test) showing that, at least in thalamus, the depolarized value of E_{GABA} is not influenced by the extrasynaptic component.

4. Discussion

The study was designed to test the hypothesis that molecular composition and functional properties of GABAergic transmission are regulated after TBI, preceding the onset of unprovoked seizures, which develop in about 25 % of the injured animals in 6 months (Kharatishvili et al., 2006; Ndode-Ekane et al., 2024). We had four major findings. First, there is a strong dysregulation of $GABA_AR$ subunit expression that appeared already 4 to 24 h after TBI, and in some cases such as for β3- and δ- subunits, persisted for up to 4 months after TBI. Second, there was a perilesional negative enrichment of GABA signaling with down-regulation of several GABA-related genes. Third, we found a dysregulation of the two main cation-chloride cotransporter genes (NKCC1 and KCC2) both in the perilesional cortex and in the ipsilateral thalamus. Fourth, the previous result was also confirmed by a GABA current reversal potential (E_{GABA}) that was shifted towards more depolarized state ipsilaterally both in the perilesional cortex and thalamus.

To this purpose, we investigated the dysregulation of GABAergic neurotransmission assessed by two well described molecular methods, *in situ* hybridization and immunohistochemistry, through a wide time window from an acute (6 h) to a chronic (4mo) post-TBI phase. For these analyses, we chose a subset of $GABA_A$ subunits, namely: those forming the α1β2γ2 isoform, which is the most abundant in the CNS and it is responsible for the synaptic fast inhibition (Chuang and Reddy, 2018); the δ subunits contained in a small percentage of the receptors, but these isoforms are mainly expressed at extrasynaptic sites and typically mediating tonic inhibitory currents (Chuang and Reddy, 2018); and β3, which recent studies suggest that, among the three beta subunits, is fundamental for proper inhibitory transmission (Nguyen and Nicoll, 2018). Thereafter, we performed the profiling analysis (mRNA-seq) at a chronic phase (3mo post-TBI) to eliminate transcriptomic changes related to the acute post-injury phase and to further reveal gene expression changes relevant to mechanisms related to evolution of post-TBI morbidities, including also epileptogenesis. One-month post-TBI time point was selected for the electrophysiological studies as our results from the molecular studies indicated a robust dysregulation of the GABAergic signaling already at 10d post-TBI when early seizures are arising. However, we aimed to characterize a phase relevant to the mechanisms of the early epileptogenesis, that is, after the acute and subacute post-TBI phase. A recent study (Boone et al., 2019) reported high overall gene-expression dysregulation still at 14d post-TBI indicated by hierarchical clustering of acute, subacute and chronic gene expression profiles after TBI. Thereafter, overall gene expression seems to return closer to normal condition, even if leaving particular pathological gene expression dysregulation still persists (*e.g.*, inflammatory signaling). Thus, existing independent molecular data (Boone et al., 2019) supports our choice of selecting a time point after the acute and subacute post-TBI phase representing well the occurrence of epileptogenesis. Moreover, after lateral fluid percussion injury (FPI), only 6–17 % of rats experience spontaneous seizures 8–15 weeks post-TBI (Kharatishvili et al., 2006) and the number of epileptic rats increases gradually overtime being 43–50 % at one-year post-TBI (Kharatishvili et al., 2006). As a summary, functional results obtained in this study represent well the phase of the epileptogenesis where studied rats did not yet have spontaneous seizures, but the brain was cleared from the gene-expression changes caused by the acute post-injury phase.

We recognize that the study of epileptogenesis in this model would have been more detailed if we also added rats that were subjected to TBI but did not develop epilepsy (TBI non-PTE) to the analysis, in order to highlight the molecular and electrophysiological changes that occur in PTE rats. However, previous studies have shown that achieving this goal is not an easy task, due to the multifocal nature of seizures in this model. This multifocality would indeed prevent a correct sampling before the monitoring and analysis of chronic EEG, limiting the possibility of correctly spotting region-selective changes (Ndode-Ekane et al., 2024). Furthermore, we and others have recently discovered that the focal area develops around the cortical lesion cavity (Ndode-Ekane, 2024). Therefore, after the decay of early seizures (D0-D7 post-injury) and evolution of cortical pathology (mostly weeks 1–3 post-injury (Immonen et al., 2009; Manninen et al., 2020), the remaining changes in the perilesional cortex will likely be relevant for late ictogenesis. Previous studies have shown regulated expression of $GABA_AR$ subunits after TBI in the neocortex, in the hippocampus and thalamus (Drexel et al., 2015; Guerriero et al., 2015; Kharlamov et al., 2011; Raible et al., 2015). In detail, Raible et al. showed decreased levels of α1 in the hippocampus at 6 h (mRNA), 24 h (protein), 48 h (protein) and 1 wk. (protein) after lateral FPI in rat. These authors also reported increased levels of α4 at 6 h (mRNA) and 24 h (protein) post-TBI. Our earlier study highlighted very similar pattern of $GABA_AR$ subunit mRNA dysregulation in the hippocampus (Drexel et al., 2015). We observed decreased levels of α1 in the dentate gyrus (6 h, 24 h and 10d post-TBI) and CA3 (6 h and 24 h post-TBI ipsilaterally). Interestingly, as others (Kharlamov et al., 2011), we also reported decreased level of γ2 in dentate gyrus (6 h post-TBI) and CA3 (6 h and 10d post-TBI). In addition, decreased level of δ was observed at 6 h and 24 h post-TBI. As a summary, subunits responsible for the phasic inhibition (α1/γ2) were down-regulated, while those responsible for the tonic inhibition (α4/δ1) were most often up-regulated. Our data are in line with previous observations and extend the previous data by showing that the $GABA_AR$ subunits dysregulation is long-lasting for at least up to 4 months. Most prominent down-regulation of $GABA_A$-R subunits were observed in an imminent relation to injury location visualized in the T2-weighted MRI images before for the used animal model (Immonen et al., 2008). Thus, compromised inhibition could contribute to both early post-injury seizures and the evolution of epileptiform activity in the perilesional cortex.

The dysregulation of $GABA_AR$ subunit expression was corroborated by the mRNA-seq and gene set enrichment analysis. We are aware that a

bulk RNA-seq analysis can only depict overall changes in the piece of the analyzed tissue lacking any spatial resolution, thus explaining the differences of the results observed between the methods used in this study. However, RNA-seq also revealed a clear alteration in the expression of NKCC1 and KCC2. These two genes possess a pivotal role in the function of inhibitory GABA currents, since it has been demonstrated that their modulation is involved both in physiological and pathological phenomena, such as epilepsy and neurodevelopmental disorders (Ben-Ari, 2002; Deidda et al., 2015; Ruffolo et al., 2018; Talos et al., 2012; Tang et al., 2016). Furthermore, previous evidence suggests that these two transporters may possess a pathogenic role also in TBI. Indeed, some of these studies suggest that early NKCC1 up-regulation during the first week after TBI may be involved in the occurrence of acute post-TBI seizure susceptibility and seizures (Wang et al., 2017). Also, KCC2 expression was reduced during the first two weeks after TBI and pharmacological enhancement of KCC2 function promoted behavioral recovery (Lizhnyak et al., 2019). Our data demonstrate that perilesional cortical dysregulated expression of NKCC1 and KCC2 persists for up to three months after TBI. Moreover, comparable transporter alteration is also found in the ipsilateral thalamus. These observations suggest a long-lasting presence of dysregulated chloride homeostasis, which can chronically impair the function of inhibitory GABA-mediated neurotransmission over the course of post-traumatic epileptogenesis. Our electrophysiological experiments further support this hypothesis, since for the first time, we recorded functional GABA-evoked currents in this TBI model, showing a depolarized E_{GABA} in the perilesional cortex and the ipsilateral thalamus. Interestingly, similar unbalances were not observed contralaterally. This alteration was also sensitive to the NKCC1 blocker bumetanide. This strengthens the hypothesis of dysregulation of chloride homeostasis post-TBI and also paves the road to targeted therapeutic interventions which could aim to restore a physiological GABAergic inhibition following brain injury (Hui et al., 2016). In the light of this interesting functional findings, we propose that TBI sets in motion a series of molecular changes, including $GABA_AR$ subunit rearrangements and chloride transporters dysfunction which ultimately produce an impairment in the electrophysiological features of GABA-evoked currents. Therefore, we can hypothesize that inhibitory neurotransmission becomes weaker, which may facilitate the spreading of epileptiform discharges and seizures (Ndode-Ekane et al., 2024).

Previous studies have reported reduction in different subtypes of cortical interneurons after lateral FPI, including those parvalbumin and somatostatin positive, corresponding to fast-spiking and non-fast-spiking interneurons, respectively (Nolan et al., 2022). Interneuron loss has also been reported after TBI in humans (Buriticá et al., 2009). Therefore, it is not surprising that in the core of the lesion, we were not able to record any functional GABAergic currents. In contrast, we found a clear alteration of inhibitory GABAergic function in both perilesional and thalamic ipsilateral regions, strengthening the hypothesis that the epileptogenic mechanisms are triggered by the altered function of the surrounding brain tissues and not by the lesion itself (Conti et al., 2011). In line with this hypothesis, we suggest that early post-TBI intervention, by restoring a normal activity of the GABAergic function, could preserve the physiological function of inhibitory neurotransmission and prevent or slow down the development of increased seizure susceptibility (Wang et al., 2017).

CRediT authorship contribution statement

Noora Puhakka: Writing – review & editing, Writing – original draft, Investigation, Formal analysis, Data curation. **Pierangelo Cifelli:** Writing – review & editing, Writing – original draft, Investigation, Funding acquisition, Formal analysis, Data curation. **Gabriele Ruffolo:** Writing – review & editing, Writing – original draft, Investigation, Funding acquisition, Formal analysis, Data curation. **Alessandro Gaeta:** Investigation, Data curation. **Cristina Roseti:** Investigation, Formal analysis, Data curation. **Angela Di Iacovo:** Investigation, Formal analysis, Data curation. **Johanna Tiilikainen:** Investigation, Formal analysis, Data curation. **Xavier Ekolle Ndode-Ekane:** Investigation, Formal analysis, Data curation. **Anssi Lipponen:** Investigation, Formal analysis, Data curation. **Meinrad Drexel:** Writing – review & editing, Writing – original draft, Investigation, Formal analysis, Data curation. **Günther Sperk:** Writing – review & editing, Writing – original draft, Investigation, Formal analysis, Data curation. **Asla Pitkänen:** Writing – review & editing, Writing – original draft, Investigation, Funding acquisition, Formal analysis, Data curation, Conceptualization. **Eleonora Palma:** Writing – review & editing, Writing – original draft, Funding acquisition, Formal analysis, Data curation, Conceptualization.

Declaration of competing interest

The authors declare that they have no known competing financial interests or personal relationships that could have appeared to influence the work reported in this paper.

Acknowledgements

We thank Mr. Jarmo Hartikainen and Mrs. Merja Lukkari for their excellent technical assistance. The study was supported by the European Union Grant FP6 EPICURE (LSH-CT-2006-037315, A.P., G.S), The Academy of Finland (Grants 272249, 338182, 273909, and 317203, A. P.), the Sigrid Juselius Foundation (A.P.). This work was supported by the Fondi Ateneo grants, grant nos. RM11916B84D24429 (EP), RG12117A8697DCF1 (EP, GR) funded by Sapienza University, AICE-FIRE 2022 (GR), PRIN 2022 (EP, GR and PC) and PRIN-PNRR 2022 (EP) from the Italian Ministry of University and Research. GR was also supported by the Italian Ministry of Health, "Ricerca corrente". PC received the intramural grant from Department of Biotechnological and Applied Clinical Sciences of the University of L' Aquila: "DISCAB grant 2024", 07_DISCAB_grant_2024.

Appendix A. Supplementary data

Supplementary data to this article can be found online at https://doi.org/10.1016/j.expneurol.2025.115183.

Data availability

Data will be made available on request.

References

Alfano, V., Romagnolo, A., Mills, J.D., Cifelli, P., Gaeta, A., Morano, A., Mühlebner, A., Aronica, E., Palma, E., Ruffolo, G., 2022. Unexpected effect of IL-1β on the function of GABAA receptors in pediatric focal cortical dysplasia. Brain Sci. 12, 807. https://doi.org/10.3390/brainsci12060807.

Andrade, P., Paananen, T., Ciszek, R., Lapinlampi, N., Pitkänen, A., 2018. Algorithm for automatic detection of spontaneous seizures in rats with post-traumatic epilepsy. J. Neurosci. Methods 307, 37–45. https://doi.org/10.1016/j.jneumeth.2018.06.015.

Ben-Ari, Y., 2002. Excitatory actions of gaba during development: the nature of the nurture. Nat. Rev. Neurosci. 3, 728–739. https://doi.org/10.1038/nrn920.

Boone, D.R., Weisz, H.A., Willey, H.E., Torres, K.E.O., Falduto, M.T., Sinha, M., Spratt, H., Bolding, I.J., Johnson, K.M., Parsley, M.A., DeWitt, D.S., Prough, D.S., Hellmich, H.L., 2019. Traumatic brain injury induces long-lasting changes in immune and regenerative signaling. PLoS One 14, e0214741. https://doi.org/10.1371/journal.pone.0214741.

Braat, S., Kooy, R.F., 2015. The GABAA receptor as a therapeutic target for neurodevelopmental disorders. Neuron 86, 1119–1130. https://doi.org/10.1016/j.neuron.2015.03.042.

Brooks-Kayal, A.R., Russek, S.J., 2012. Regulation of GABAA receptor gene expression and epilepsy. In: Noebels, J.L., Avoli, M., Rogawski, M.A., Olsen, R.W., Delgado-Escueta, A.V. (Eds.), Jasper's Basic Mechanisms of the Epilepsies. National Center for Biotechnology Information (US), Bethesda (MD).

Buriticá, E., Villamil, L., Guzmán, F., Escobar, M.I., García-Cairasco, N., Pimienta, H.J., 2009. Changes in calcium-binding protein expression in human cortical contusion tissue. J. Neurotrauma 26, 2145–2155. https://doi.org/10.1089/neu.2009.0894.

Chuang, S.-H., Reddy, D.S., 2018. Genetic and molecular regulation of Extrasynaptic GABA-A receptors in the brain: therapeutic insights for epilepsy. J. Pharmacol. Exp. Ther. 364, 180–197. https://doi.org/10.1124/jpet.117.244673.

Conti, L., Palma, E., Roseti, C., Lauro, C., Cipriani, R., de Groot, M., Aronica, E., Limatola, C., 2011. Anomalous levels of Cl- transporters cause a decrease of GABAergic inhibition in human peritumoral epileptic cortex. Epilepsia 52, 1635–1644. https://doi.org/10.1111/j.1528-1167.2011.03111.x.

Deidda, G., Parrini, M., Naskar, S., Bozarth, I.F., Contestabile, A., Cancedda, L., 2015. Reversing excitatory GABAAR signaling restores synaptic plasticity and memory in a mouse model of down syndrome. Nat. Med. 21, 318–326. https://doi.org/10.1038/nm.3827.

Drexel, M., Puhakka, N., Kirchmair, E., Hörtnagl, H., Pitkänen, A., Sperk, G., 2015. Expression of GABA receptor subunits in the hippocampus and thalamus after experimental traumatic brain injury. Neuropharmacology 88, 122–133. https://doi.org/10.1016/j.neuropharm.2014.08.023.

Dulla, C.G., Pitkänen, A., 2021. Novel approaches to prevent epileptogenesis after traumatic brain injury. Neurotherapeutics 18, 1582–1601. https://doi.org/10.1007/s13311-021-01119-1.

Eusebi, F., Palma, E., Amici, M., Miledi, R., 2009. Microtransplantation of ligand-gated receptor-channels from fresh or frozen nervous tissue into Xenopus oocytes: a potent tool for expanding functional information. Prog. Neurobiol. 88, 32–40. https://doi.org/10.1016/j.pneurobio.2009.01.008.

Golub, V.M., Reddy, D.S., 2022. Post-traumatic epilepsy and comorbidities: advanced models, molecular mechanisms, biomarkers, and novel therapeutic interventions. Pharmacol. Rev. 74, 387–438. https://doi.org/10.1124/pharmrev.121.000375.

Grabenstatter, H.L., Cogswell, M., Cruz Del Angel, Y., Carlsen, J., Gonzalez, M.I., Raol, Y. H., Russek, S.J., Brooks-Kayal, A.R., 2014. Effect of spontaneous seizures on GABAA receptor α4 subunit expression in an animal model of temporal lobe epilepsy. Epilepsia 55, 1826–1833. https://doi.org/10.1111/epi.12771.

Guerriero, R.M., Giza, C.C., Rotenberg, A., 2015. Glutamate and GABA imbalance following traumatic brain injury. Curr. Neurol. Neurosci. Rep. 15, 27. https://doi.org/10.1007/s11910-015-0545-1.

Hiltunen, J., Ndode-Ekane, X.E., Lipponen, A., Drexel, M., Sperk, G., Puhakka, N., Pitkänen, A., 2021. Regulation of Parvalbumin Interactome in the perilesional cortex after experimental traumatic brain injury. Neuroscience 475, 52–72. https://doi.org/10.1016/j.neuroscience.2021.08.018.

van Hugte, E.J.H., Schubert, D., Nadif Kasri, N., 2023. Excitatory/inhibitory balance in epilepsies and neurodevelopmental disorders: depolarizing γ-aminobutyric acid as a common mechanism. Epilepsia 64, 1975–1990. https://doi.org/10.1111/epi.17651.

Hui, H., Rao, W., Zhang, L., Xie, Z., Peng, C., Su, N., Wang, K., Wang, L., Luo, P., Hao, Y., Zhang, S., Fei, Z., 2016. Inhibition of Na(+)-K(+)-2Cl(−) Cotransporter-1 attenuates traumatic brain injury-induced neuronal apoptosis via regulation of Erk signaling. Neurochem. Int. 94, 23–31. https://doi.org/10.1016/j.neuint.2016.02.002.

Immonen, R.J., Kharatishvili, I., Niskanen, J.-P., Gröhn, H., Pitkänen, A., Gröhn, O.H.J., 2009. Distinct MRI pattern in lesional and perilesional area after traumatic brain injury in rat–11 months follow-up. Exp. Neurol. 215, 29–40. https://doi.org/10.1016/j.expneurol.2008.09.009.

Kharatishvili, I., Nissinen, J.P., McIntosh, T.K., Pitkänen, A., 2006. A model of posttraumatic epilepsy induced by lateral fluid-percussion brain injury in rats. Neuroscience 140, 685–697. https://doi.org/10.1016/j.neuroscience.2006.03.012.

Kharlamov, E.A., Lepsveridze, E., Meparishvili, M., Solomonia, R.O., Lu, B., Miller, E.R., Kelly, K.M., Mtchedlishvili, Z., 2011. Alterations of GABA(A) and glutamate receptor subunits and heat shock protein in rat hippocampus following traumatic brain injury and in posttraumatic epilepsy. Epilepsy Res. 95, 20–34. https://doi.org/10.1016/j.eplepsyres.2011.02.008.

Lipponen, A., Paananen, J., Puhakka, N., Pitkänen, A., 2016. Analysis of post-traumatic brain injury gene expression signature reveals tubulins, Nfe2l2, Nfkb, Cd44, and S100a4 as treatment targets. Sci. Rep. 6, 31570. https://doi.org/10.1038/srep31570.

Lizhnyak, P.N., Muldoon, P.P., Pilaka, P.P., Povlishock, J.T., Ottens, A.K., 2019. Traumatic brain injury temporal proteome guides KCC2-targeted therapy. J. Neurotrauma 36, 3092–3102. https://doi.org/10.1089/neu.2019.6415.

Manninen, E., Chary, K., Lapinlampi, N., Andrade, P., Paananen, T., Sierra, A., Tohka, J., Gröhn, O., Pitkänen, A., 2020. Early increase in cortical T2 relaxation is a prognostic biomarker for the evolution of severe cortical damage, but not for Epileptogenesis, after experimental traumatic brain injury. J. Neurotrauma 37, 2580–2594. https://doi.org/10.1089/neu.2019.6796.

McIntosh, T.K., Vink, R., Noble, L., Yamakami, I., Fernyak, S., Soares, H., Faden, A.L., 1989. Traumatic brain injury in the rat: characterization of a lateral fluid-percussion model. Neuroscience 28, 233–244. https://doi.org/10.1016/0306-4522(89)90247-9.

Miledi, R., Eusebi, F., Martínez-Torres, A., Palma, E., Trettel, F., 2002. Expression of functional neurotransmitter receptors in Xenopus oocytes after injection of human brain membranes. Proc. Natl. Acad. Sci. USA 99, 13238–13242. https://doi.org/10.1073/pnas.192445299.

Ndode-Ekane, X.E., Ali, I., Santana-Gomez, C., Andrade, P., Immonen, R., Casillas-Espinosa, P., Paananen, T., Manninen, E., Puhakka, N., Smith, G., Brady, R.D., Silva, J., Braine, E., Hudson, M., Yamakawa, G.R., Jones, N.C., Shultz, S.R., Harris, N., Wright, D.K., Gröhn, O., Staba, R., O'Brien, T.J., Pitkänen, A., 2024. Epilepsy phenotype and its reproducibility after lateral fluid percussion-induced traumatic brain injury in rats: multicenter EpiBioS4Rx study project 1. Epilepsia 65, 511–526. https://doi.org/10.1111/epi.17838.

Nguyen, Q.-A., Nicoll, R.A., 2018. The GABAA receptor β subunit is required for inhibitory transmission. Neuron 98, 718–725.e3. https://doi.org/10.1016/j.neuron.2018.03.046.

Nolan, A.L., Sohal, V.S., Rosi, S., 2022. Selective inhibitory circuit dysfunction after chronic frontal lobe contusion. J. Neurosci. 42, 5361–5372. https://doi.org/10.1523/JNEUROSCI.0097-22.2022.

Palma, E., Trettel, F., Fucile, S., Renzi, M., Miledi, R., Eusebi, F., 2003. Microtransplantation of membranes from cultured cells to Xenopus oocytes: a method to study neurotransmitter receptors embedded in native lipids. Proc. Natl. Acad. Sci. USA 100, 2896–2900. https://doi.org/10.1073/pnas.0438006100.

Palma, E., Amici, M., Sobrero, F., Spinelli, G., Di Angelantonio, S., Ragozzino, D., Mascia, A., Scoppetta, C., Esposito, V., Miledi, R., Eusebi, F., 2006. Anomalous levels of cl- transporters in the hippocampal subiculum from temporal lobe epilepsy patients make GABA excitatory. Proc. Natl. Acad. Sci. USA 103, 8465–8468. https://doi.org/10.1073/pnas.0602979103.

Palma, E., Roseti, C., Maiolino, F., Fucile, S., Martinello, K., Mazzuferi, M., Aronica, E., Manfredi, M., Esposito, V., Cantore, G., Miledi, R., Simonato, M., Eusebi, F., 2007. GABA(A)-current rundown of temporal lobe epilepsy is associated with repetitive activation of GABA(A) "phasic" receptors. Proc. Natl. Acad. Sci. USA 104, 20944–20948. https://doi.org/10.1073/pnas.0710522105.

Raible, D.J., Frey, L.C., Del Angel, Y.C., Carlsen, J., Hund, D., Russek, S.J., Smith, B., Brooks-Kayal, A.R., 2015. JAK/STAT pathway regulation of GABAA receptor expression after differing severities of experimental TBI. Exp. Neurol. 271, 445–456. https://doi.org/10.1016/j.expneurol.2015.07.001.

Ruffolo, G., Iyer, A., Cifelli, P., Roseti, C., Mühlebner, A., van Scheppingen, J., Scholl, T., Hainfellner, J.A., Feucht, M., Krsek, P., Zamecnik, J., Jansen, F.E., Spliet, W.G.M., Limatola, C., Aronica, E., Palma, E., 2016. Functional aspects of early brain development are preserved in tuberous sclerosis complex (TSC) epileptogenic lesions. Neurobiol. Dis. 95, 93–101. https://doi.org/10.1016/j.nbd.2016.07.014.

Ruffolo, G., Cifelli, P., Roseti, C., Thom, M., van Vliet, E.A., Limatola, C., Aronica, E., Palma, E., 2018. A novel GABAergic dysfunction in human Dravet syndrome. Epilepsia. https://doi.org/10.1111/epi.14574.

Smedley, D., Haider, S., Ballester, B., Holland, R., London, D., Thorisson, G., Kasprzyk, A., 2009. BioMart–biological queries made easy. BMC Genomics 10, 22. https://doi.org/10.1186/1471-2164-10-22.

Sperk, G., Schwarzer, C., Tsunashima, K., Fuchs, K., Sieghart, W., 1997. GABA(A) receptor subunits in the rat hippocampus I: immunocytochemical distribution of 13 subunits. Neuroscience 80, 987–1000. https://doi.org/10.1016/s0306-4522(97)00146-2.

Subramanian, A., Tamayo, P., Mootha, V.K., Mukherjee, S., Ebert, B.L., Gillette, M.A., Paulovich, A., Pomeroy, S.L., Golub, T.R., Lander, E.S., Mesirov, J.P., 2005. Gene set enrichment analysis: a knowledge-based approach for interpreting genome-wide expression profiles. Proc. Natl. Acad. Sci. USA 102, 15545–15550. https://doi.org/10.1073/pnas.0506580102.

Talos, D.M., Sun, H., Kosaras, B., Joseph, A., Folkerth, R.D., Poduri, A., Madsen, J.R., Black, P.M., Jensen, F.E., 2012. Altered inhibition in tuberous sclerosis and type IIb cortical dysplasia. Ann. Neurol. 71, 539–551. https://doi.org/10.1002/ana.22696.

Tang, X., Kim, J., Zhou, L., Wengert, E., Zhang, L., Wu, Z., Carromeu, C., Muotri, A.R., Marchetto, M.C.N., Gage, F.H., Chen, G., 2016. KCC2 rescues functional deficits in human neurons derived from patients with Rett syndrome. Proc. Natl. Acad. Sci. USA 113, 751–756. https://doi.org/10.1073/pnas.1524013113.

Tsunashima, K., Schwarzer, C., Kirchmair, E., Sieghart, W., Sperk, G., 1997. GABA(A) receptor subunits in the rat hippocampus III: altered messenger RNA expression in kainic acid-induced epilepsy. Neuroscience 80, 1019–1032. https://doi.org/10.1016/s0306-4522(97)00144-9.

Wang, F., Wang, X., Shapiro, L.A., Cotrina, M.L., Liu, W., Wang, E.W., Gu, S., Wang, W., He, X., Nedergaard, M., Huang, J.H., 2017. NKCC1 up-regulation contributes to early post-traumatic seizures and increased post-traumatic seizure susceptibility. Brain Struct. Funct. 222, 1543–1556. https://doi.org/10.1007/s00429-016-1292-z.